Available online at www.sciencedirect.com
ScienceDirect
International Journal of Mass Spectrometry 255–256 (2006) 28–38
International Journal of Mass Spectrometry
www.elsevier.com/locate/ijms

Nitrosamide, (H_2NNO), formation within $[(NO)_m(NH_3)_n]^+$ clusters: Theory and experiment

Dong Nam Shin [b], Marek Freindorf [c], Thomas R. Furlani [c], Robert L. DeLeon [a], James F. Garvey [a,*]

[a] *Department of Chemistry, University at Buffalo, State University of New York at Buffalo, Buffalo, NY 14260-3000, USA*
[b] *Research Institute of Industrial Science and Technology, P.O. Box 135, Pohang 790-600, South Korea*
[c] *Center for Computational Research, University at Buffalo, State University of New York at Buffalo, Buffalo, NY, USA*

Received 8 July 2005; received in revised form 16 September 2005; accepted 19 September 2005
Available online 16 November 2005

Abstract

The generation of nitrosamide (H_2NNO) molecules mediated by the cluster environment of the NO/NH_3 cluster system has been explored, employing both multiphoton ionization time-of-flight mass spectrometry and ab initio calculations. This combined approach indicates that the H_2NNO species is viable and can exist within cluster ions of the type $[H_2NNO\cdots NO\cdots NH_3]^+$. Possible mechanisms for formation of the H_2NNO species are discussed.

Keywords: Gas phase clusters; Ion–molecule chemistry; Nitric oxide; Ammonia; Nitrosamide

1. Introduction

Among air pollutants, nitrogen oxides (NO_x) have received particular attention because of their crucial role in many global environmental problems [1–3], i.e., acid rain and photochemical smog formation. There is great interest in the development of technologies that can be applied to removing nitrogen oxides ($DeNO_x$) from the exhaust of coal-fired power plants, steel sintering plants, oil boilers and diesel engines. These technologies include selective non-catalytic reduction (SNCR) [4–8], selective catalytic reduction (SCR) [9–12] and non-thermal plasma (NTP) [13,14] processes. In addition, a hybrid process that utilizes a combination of these techniques also has been developed [15–17]. It is worth noting that all these various technologies involve in common the injection of gaseous ammonia (NH_3) for the reduction of NO_x in SCR and SNCR, and for the neutralization of nitric acids generated in the NTP processes.

In the flue gas cleaning, gas phase cluster and heterogeneous chemical reactions significantly dominate [18–21]. For example, the efficiency of $DeNO_x$ is greatly enhanced when water vapor exists in the flue gas mixture and is considered to be primarily due to the formation of both $NO^+(H_2O)_n$ and $NO_2^+(H_2O)_n$ clusters [22–24]. The chemically active species (CAS) in the NTP process, include radicals, ions and highly excited molecules that are generated by the NTP discharge [13,14]. In CAS, the OH radicals are significantly involved in the removal of air pollutants and come from the dissociation of cluster ions, such as $O_2^+(H_2O)_2$ and $(H_2O)_2^+$ through the ion–molecule reaction of O_2^+ with water [25]. In the ionic $DeNO_x$ mechanism, examined by Egsgaard et al. [26], the key to this process is the formation of the $NO^+\cdots NH_3$ complex in the CH_4/NH_3 flame. Subsequently, this complex may react with either ammonia or water to produce nitrosamide (H_2NNO), which is also known to an important intermediate responsible for removing NO_x in SNCR process [4,5,8]. The reduction of NO_x has been observed by Richter et al. [27] in the SCR process using NH_4^+ ions fixed in zeolites. In the atmosphere, ions may also involve nucleation despite the low atmospheric concentrations [28–30] because the charge significantly facilitates the stabilization of the small clusters relative to the neutral counterparts. The study by Yu et al. [31] has showed that rapid aerosol formation and growth observed in aircraft exhaust plumes are due to ions. Therefore, investigation of the chemical reactions occurring within the cluster ions containing atmospheric species and additives for $DeNO_x$ processes, i.e.,

* Corresponding author.
E-mail address: garvey@buffalo.edu (J.F. Garvey).

1387-3806/$ – see front matter © 2005 Elsevier B.V. All rights reserved.
doi:10.1016/j.ijms.2005.09.006

NO, NH_3, H_2O, alcohols, etc., will aid in the understanding of the fundamental ion chemistry occurring in the $DeNO_x$ process as well as in the upper atmosphere.

Previous experiments have reported observation [32–34] of chemical reactivity of NO cluster ions toward molecules containing a hydroxyl group (i.e., CH_3OH, C_2H_5OH, C_3H_7OH and C_4H_9OH). This suggests that alcohols might also be employed as an additive to improve the efficiency of the $DeNO_x$ processes [7,35]. For example, in the NO/CD_3OH system [32], the formation of CD_3ONO molecules within cluster ions is the dominant process, and is very dependant on both the number of NO molecules and the overall electron configuration of the cluster ion. The NO/C_2H_5OH cluster system is also of interest [33] in that if the concentration of ethanol in the gas mixture, prior to expansion into the vacuum chamber, is above a certain critical value, preference is shown for loss of hydroxyl hydrogen. However, below a critical value of ethanol concentration, the hydrogen loss now occurs at the α-carbon. This competitive switching pattern in the position of the hydrogen atom loss against the ethanol concentration is thought to be controlled by the degree of the hydrogen-bonding network within cluster ions. In cases where mixed clusters of NO/ROH (ROH = C_2H_5OH, C_3H_7OH and C_4H_9OH) are used [34], the formation of the product cluster ions having RONO species is predominantly observed as a major series. Based on this past work, it is interesting to speculate on whether the chemical reaction within NO/NH_3 clusters occurs in a manner similar to that within NO/ROH clusters.

Since NH_3 serves as the reductant as well as the neutralizer for $DeNO_x$ process, we have now investigated chemical reactions taking place within the cluster ions of the form $[(NO)_m(NH_3)_n]^+$. This present work is concentrated on the possibility of whether there is a special chemical reactivity of the NO clusters towards the N–H bond of NH_3, similar to the previous chemistry we observed with NO and molecules containing a hydroxyl group. We anticipate that the formation of nitrosamide (H_2NNO) species may occur within $[(NO)_m(NH_3)_n]^+$ clusters. The formed H_2NNO 'intermediate' could then dissociate directly into N_2 and H_2O [4]. We have also performed ab initio molecular orbital (MO) calculations in order to aid in understanding the structures, energies and charge distributions of clusters containing H_2NNO species.

2. Experimental

A detailed description of the reflectron time-of-flight mass spectrometer (RTOFMS) instrument has been provided elsewhere [36,37]. In brief, the neutral heteroclusters were expanded through a pulsed nozzle (General Valve Co., IOTA ONE) with an 800 μm orifice diameter. After skimming the expansion with a 1.0 mm conical skimmer located 1.5 cm away from the nozzle, the cluster beam was then introduced into the ionization region of the RTOFMS and irradiated by the unfocused 248 nm pulsed laser beam (Lambda Physik, EMG101), with typical laser energy below 3.5 mJ $pulse^{-1}$. Cluster ions generated by the laser were accelerated in a double electrostatic field to 4.2 keV and travel through a 140 cm long flight tube before being reflected by a double stage reflectron (R.M. Jordan Co.) located at the top of the flight tube. Following the reflectron, the ions traveled an additional 61 cm to a dual microchannel plate (MCP) detector. The background pressure in the flight tube of the mass spectrometer was maintained below 5×10^{-7} Torr to reduce any collision induced dissociation processes by using both a 370 L/s turbo molecular pump and liquid nitrogen trap. The pressure of the ionization region rises to 5×10^{-6} Torr during the normal operation. The detected ion signals were recorded by a transient digitizer (LeCroy 9310).

In the cluster expansions, experiments are typically performed with a gas mixture consisting of 0.24–1.28% ammonia and 5.0% nitric oxide in 2.4 atm Ar carrier gas. The 99.99% (anhydrous grade) ammonia gas was obtained from Linde Specialty Gases. The 5.0% nitric oxide gas (seeded in Ar) was obtained from Matheson Gases. All of these reagents were used without further purification.

3. Experimental results

Fig. 1 shows a survey mass spectra of NO/NH_3 mixed cluster ions taken at two different concentrations of NH_3 seeded in Ar containing NO of 5%. Under high concentration of NH_3 (1.24% NH_3 and 5% NO), as shown in Fig. 1(a), the heterocluster ion series corresponding to $[(NO)(NH_3)_n]^+$, denoted by (1,n), are observed to be the most prominent mixed cluster ion peaks. A series of neat protonated ammonia clusters $(NH_3)_nH^+$, are also observed and represented by A_n. In previous work [37], we observed that the mixed cluster ions, $[(NO)(NH_3)_n]^+$, can be considered as having a structure where the ion core NO^+ is solvated by the ammonia molecules. This picture of NO^+ solvated by NH_3 is different from that for the mixed cluster ion $[(NO)(H_2O)_n]^+$ [38,39] where the structure of $[NO(H_2O)_n]^+$ cluster ion depends on the cluster sizes n; for $n \leq 3$, the ion core is NO solvated by water molecules, while, for $n \geq 4$, the $[NO(H_2O)_n]^+$ the cluster ion now exists in the form $(H_2O)_{n-1}H^+ \cdot HONO$. Ab initio calculations [40] have also borne out structural changes with an increased number of water molecules within the cluster ions.

In our study, we find that mixed cluster ions containing two (or more) NO molecules are not easily observed, regardless of the mixing ratio of NO to NH_3 concentrations in the gas mixture prior to expansion. While the intensity of the homogeneous NO cluster ions is significantly enhanced by a low concentration of NH_3, mixed cluster ion peaks of the type $[(NO)_{m>1}(NH_3)_n]^+$ are not increased substantially. However, cluster ions corresponding to $[(NO)(NH_3)_n]^+$ and $(NH_3)_nH^+$ are still detected regardless of the expansion condition. This result differs from previous work [32,33] on NO/ROH clusters at comparable experimental conditions, where the heterocluster ions were found to be significantly more abundant than the corresponding homogeneous cluster ions $(NO)_m^+$ and $(ROH)_nH^+$. It was also observed that for the NO/CH_3OH system predominant formation of the heterogeneous cluster ions $[(NO)(CH_3ONO)_x]$ (x = 1–12), and cluster ions, such as $(NO)_m^+$ (for $m > 3$) and $(CH_3OH)_nH^+$ (for $n > 3$) are not seen [41]. These results imply fundamental differences between the NO/ROH and NO/NH_3 systems.

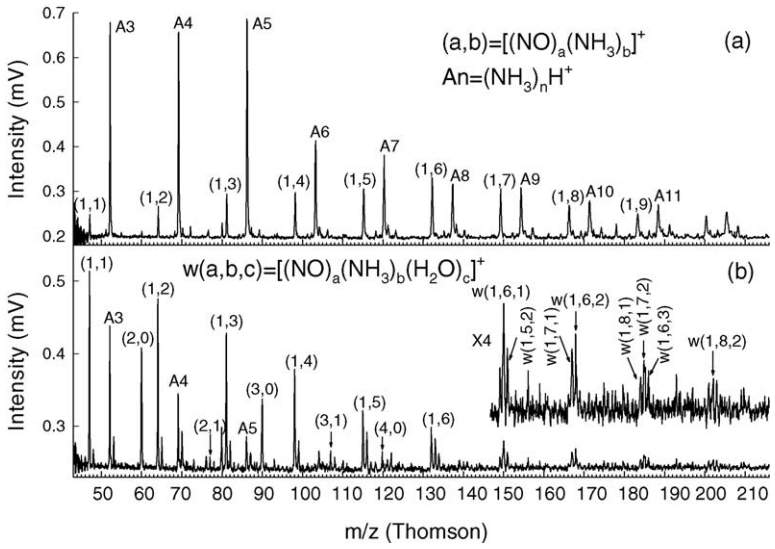

Fig. 1. Typical mass spectra: (a) NO (5%) and NH_3 (1.28%) and (b) NO (5%) and NH_3 (0.24%) mixed cluster seeded in 2.4 atm of Ar carrier gas. The series of protonated parent ammonia cluster ions of the form $(NH_3)_nH^+$ is designated by A_n. The mixed cluster ion series of the form $[(NO)_m(NH_3)_n]^+$ are designated by $a(m,n)$. The three component mixed cluster ions of the form $[(NO)_m(H_2O)_x(NH_3)_n]^+$ are designated by $w(m, x, n)$, respectively.

This effort can lend some insight into the chemical reactivity of NO cluster ions with NH_3 to generate the H_2NNO species within clusters (similar to the generation of RONO in the NO/ROH system [32–34,41]). We had observed in our previous studies of NO/ROH clusters [32–34,41], that the formation of the RONO species seems to require at least two or more NO molecules within the initial heterocluster ion (i.e., $[(NO)_{m>1}(CH_3OH)_n]^+$). Can this same behavior be observed with NO/NH_3 clusters?

For a gas mixture of 0.24% NH_3 and 5.0% NO in Ar, the survey mass spectrum is displayed in Fig. 1(b). The intensity of both the $(NO)_m^+$, and $(NO)(NH_3)_n^+$ clusters ions are observed to be enhanced in comparison to Fig. 1(a). While the generation of mixed clusters comprising two or three NO molecules, such as $[(NO)_2(NH_3)]^+$ and $[(NO)_3(NH_3)]^+$ are found to be only marginally enhanced. The $[(NO)(NH_3)_n]^+$ cluster ions are now split into sets of peaks spaced by a 1 amu mass difference. We believe these additional peaks are attributed to the presence of water that may arise from the dissociation of the H_2NNO formed within the cluster ion, which is discussed at the end of this section.

Fig. 2(a) shows the mass range between the $[(NO)_2(NH_3)]^+$ and $[(NO)_3(NH_3)]^+$ cluster ions. Cluster peaks containing the H_2NNO species, are indicated by a closed circle, and are assigned as $[(NO)(H_2NNO)_x(NH_3)_{n-x}]^+$ peaks where $x = 1$ or 2. We also note that $[(H_2NNO)(NH_3)_{n-1}]^+$ ions have not been

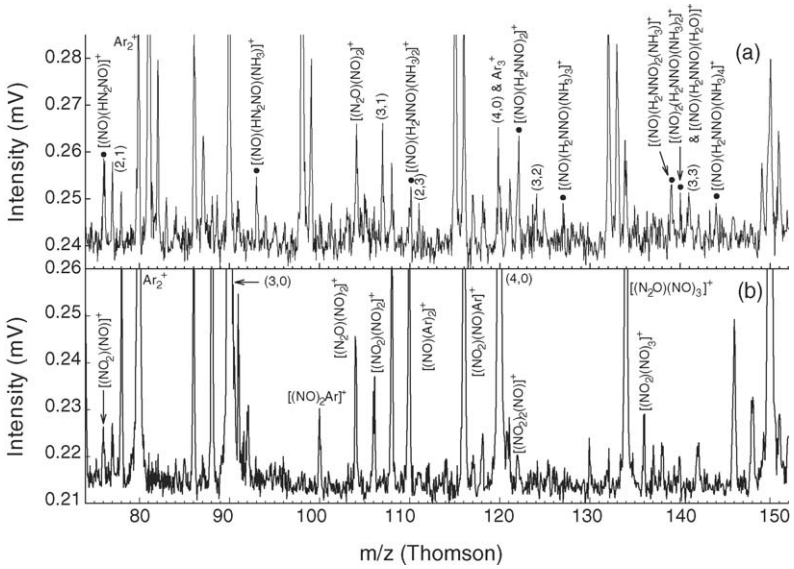

Fig. 2. A comparison of expanded mass spectra showing the formation of the H_2NNO species with that obtained from pure the NO cluster system: (a) NO (5%) and NH_3 (0.24%) in Ar of 2.4 atm and (b) NO (5%) in Ar of 2.4 atm. Experimental conditions are identical in both cases. Both mass spectra were plotted with the same scale on the *X*- and *Y*-axis, in order to compare the features of the two mass spectra. The peaks containing the H_2NNO species are marked with a closed circle (●).

observed, even though the major mixed cluster series in all mass spectra is found to be $[(NO)(NH_3)_n]^+$. We observe the generation of H_2NNO only in mixed cluster ions possessing two or more NO molecules, which is similar to NO/ROH system [32–34,41].

We note that the mass of H_2NNO is equivalent to that of NO_2 and peaks that we have assigned to clusters containing H_2NNO species could also be identified as being the NO_2 species. To try and verify our original assignment, we have studied 5% NO in Ar in the absence of ammonia but under otherwise identical conditions [42]. This spectrum is shown in Fig. 2(b), with both the same mass range and intensity scale as in Fig. 2(a). The neat NO cluster spectra does show a series of small peaks containing NO_2 species $[(NO)_{m=1-3}(NO_2)]^+$ as mentioned above [42]. Since the NO_2 molecule possesses an unpaired electron, forming even-electron configuration ions dominates. As a result, one observes an even–odd intensity alteration within the cluster ions, similar to that of pure NO cluster ions [43]. Indeed, the intensity of the $[(NO)_2(NO_2)]^+$ cluster in Fig. 2(b) is relatively large compared to that of either the $[(NO)_1(NO_2)]^+$ or the $[(NO)_3(NO_2)]^+$ cluster ions. However, this alteration is in marked contrast with Fig. 2(a), where the intensity of the peaks corresponding to $[(NO)_2(NO_2)]^+$ and $[(NO)_3(NO_2)]^+$ clusters are nearly suppressed, and only the peak at the mass corresponding to $[(NO)_1(NO_2)]^+$, which is also at the same mass as the $[(NO)(H_2NNO)]^+$ cluster, appears somewhat enhanced. Such a difference in mass spectra between pure NO and NH_3/NO systems, we believe, strengthens our assignment for the $[(NO)(H_2NNO)_x(NH_3)_{n-x}]^+$ cluster ions in Fig. 2(a).

In an attempt to help identify the formation of H_2NNO within these NO/NH_3 clusters, we did try to use isotopically substituted ammonia, ND_3. However, accidental mass coincidences due to isotope scrambling leads to a multitude of peaks spaced by 1 amu, severely complicating any further analysis (i.e., $[(NO)(ND_3)_3]^+$, $[(NO)(ND_2H)(ND_3)_2]^+$ and $[(NO)(ND_2H)_2(ND_3)]^+$).

When the ammonia concentration is decreased, the mixed cluster ion series $[(NO)(NH_3)_n]^+$ is separated into two or more peaks at the high mass region with 1 amu mass difference, as shown in Fig. 1(b). The intensity of these additional peaks is pronounced in comparison to the $[(NO)(NH_3)_n]^+$ ions in the high mass region. These peaks can be explained by the incorporation of water leading to cluster ions of the form $[(NO)(H_2O)_x(NH_3)_{n-x}]^+$ ion. We also note that these cluster ions have the same mass to charge ratio as their protonated form, $[(NO)(H_2O)_{x-1}(NH_3)_{n-x+1}]H^+$ cluster ions. However, it appears to be unlikely that such protonated cluster ions are formed within clusters because we saw no evidence supporting the formation of the protonated form in our previous study of NO/NH_3 [37] and NO/ROH [32–34,41] systems, even though protonated cluster ions such as $(NH_3)_nH^+$ and $(CH_3OH)_nH^+$ are mainly observed when NH_3 and CH_3OH, respectively, are expanded.

There are two possibilities that might account for H_2O within the cluster ions, as observed in Fig. 1(a): (1) it could be present due to water impurities from both the gas samples and the vacuum chamber and (2) it might arise from intracluster ion–molecule reactions. In this study, we have used 99.99% anhydrous grade NH_3. In separate mass spectra of both the homogeneous NO and NH_3 systems, the intensity of the cluster ions including water molecules is negligible in comparison with that of the $(NO)_n^+$ and $(NH_3)_nH^+$ cluster ions. While it is difficult to completely rule out the influence of water impurities failure to observe it in neat expansions would suggest a different source for its generation. After its formation, H_2NNO may undergo subsequent dissociation, leading to the formation of H_2O and N_2. We believe, at least in part, that the observation of clusters containing water, occurs through the dissociation of the H_2NNO species. We have proposed a possible reaction mechanism for both the formation of the H_2NNO species and its subsequent dissociation into H_2O and N_2 (Scheme 1). This mechanism is consistent with results that H_2NNO is viable within clusters with a lifetime in the microsecond regime [44,45]. The H_2NNO cluster ion may then be either stabilized (via cluster solvation) or dissociate to generate H_2O plus N_2, where the water is then retained within the cluster.

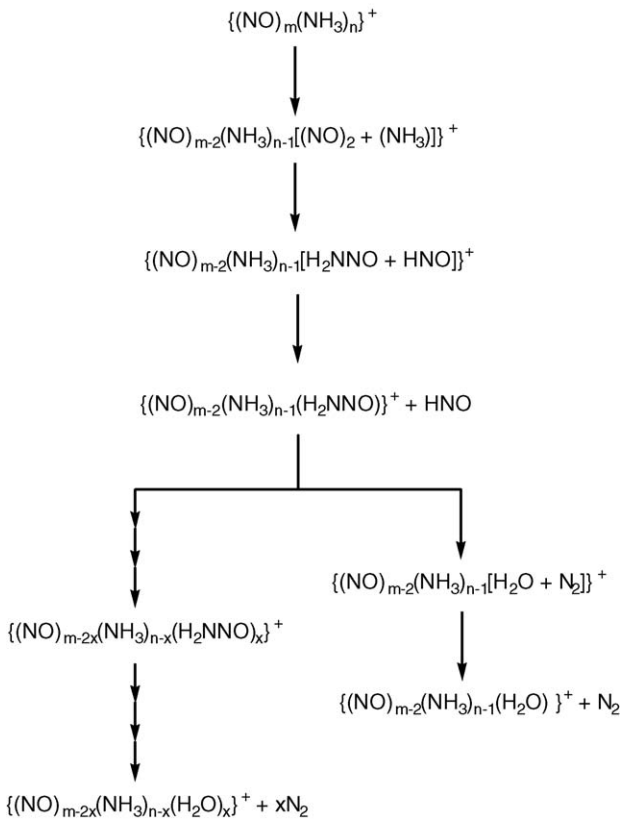

Scheme 1.

4. Calculated energies and geometries

In order to better understand the structures and relative energetics of the observed cluster ions involving H_2NNO molecules, we have performed quantum chemical calculations on the $[(NO)_2(NH_2)]^+$ ion. In this study, we found that the NH_2 radical reacts with the $(NO)_2^+$ dimer ion to generate the complex ion $[NO\cdots H_2NNO]^+$ with little or no activation energy barrier. These calculations also support the observation of cluster ions

Table 1
Calculated properties of monomers[a]

Properties	NO	NO^+	H_2NNO	H_2NNO^+
Energy	−129.5589003	−129.2425865	−185.3521126	−185.0050291
E(ZPVE)[b]	5.20	2.81	19.42	20.33
R(NO)	1.143	1.103	1.237	1.148
R(NN)			1.342	1.280
$R(NH_1)$			1.013	1.024
$R(NH_2)$			1.005	1.017
∠ONN			112.9	136.5
$\angle H_1NN$			118.0	118.9
$\angle H_2NN$			116.1	116.7
$\angle H_1NNO$			9.6	0.0
$\angle H_2NNO$			168.8	180.0
q(O)	−0.196	0.238	−0.429	−0.023
q(N)	0.196	0.762	0.261	0.496
q(N)			−0.486	−0.358
$q(H_1)$			0.324	0.437
$q(H_2)$			0.330	0.450

[a] UMP2/6-31G(d,p) results where the total energies in hartrees, the bond lengths in Å, the bond angles in degrees and atomic charges in e are used.
[b] ZPVE (scaled by 0.93).

losing an H atom from NH_3 to form the complex ion (i.e., $[(NO)_2\cdots(NH_2)]^+ \rightarrow [NO\cdots H_2NNO]^+$).

Optimized geometries and zero-point vibrational energies (ZPVE) were obtained from unrestricted second order Møller-Plesset perturbation theory (UMP2) using a standard 6-31G(d,p) basis set and the electronic structure program GAUSSIAN 94 [46]. All ZPVE were scaled by 0.93 to account for the fact that vibrational frequencies calculated at the MP2 level are known to be too large [47]. All reaction energies were corrected for ZPVE and basis set superposition error (BSSE) using the counter poise correction [48].

Calculations on possible forms of the $[NO\cdots H_2NNO]^+$ ion complex (namely NO, NO^+, H_2NNO and H_2NNO^+), were carried out to provide a basis of comparison with complex ions. Total energies, geometrical parameters and Mulliken atomic charges for monomers are presented in Table 1. Ionization of H_2NNO is accompanied by a change in symmetry from C_1 (non-planar) to C_s (planar).

Five different structures of the $[NO\cdots H_2NNO]^+$ ion complex possessing C_s symmetry are shown in Fig. 3. Table 2 presents the Mulliken charge density analysis of these complex ions and reveals that the charge distribution of the NH_2NO moiety in the complex ions is close to that of the isolated NH_2NO neutral molecule (in Table 1), while the charge distribution of the NO moiety in the complex ion is similar to that of the isolated NO^+ ion. The percentage of the total charge of +1 residing on the

Table 2
Calculated properties of complexes[a]

Properties	C1	C2	C3	C4	C5
Energy	−314.6563161	−314.6386402	−314.6539411	−314.6587514	−314.6416251
E(ZPVE)[b]	24.55	23.83	24.73	24.49	24.20
$R(O_1N_1)$	1.127	1.119	1.136	1.129	1.127
$R(N_1O_2)$	1.971	$R(O_1O_2) = 2.145$	$R(N_1N_2) = 2.213$	2.024	2.036
$R(O_2N_2)$	1.270	1.258	1.228	1.255	1.254
$R(N_2N_3)$	1.285	1.300	1.295	1.288	1.290
$R(N_3H_1)$	1.020	1.018	1.019	1.020	1.013
$R(N_3H_2)$	1.013	1.010	1.011	1.013	1.018
$\angle O_1N_1O_2$	109.4	$\angle N_1O_1O_2 = 114.7$	$\angle O_1N_1N_2 = 87.6$	106.0	96.9
$\angle N_1O_2N_2$	112.9	$\angle O_1O_2N_2 = 102.9$	$\angle N_1N_2N_3 = 145.3$	98.0	137.6
$\angle O_2N_2N_3$	112.9	113.6	119.8	114.7	117.2
$\angle N_2N_3H_1$	121.1	120.4	119.8	120.9	123.1
$\angle N_2N_3H_2$	116.1	116.6	117.0	116.3	115.3
$q(O_1)$	0.085	0.219	0.158	0.094	0.139
$q(N_1)$	0.664	0.685	0.621	0.657	0.637
$q(O_2)$	−0.490	−0.533	−0.371	−0.454	−0.513
$q(N_2)$	0.318	0.286	0.207	0.286	0.384
$q(N_3)$	−0.368	−0.406	−0.370	−0.373	−0.407
$q(H_1)$	0.391	0.370	0.395	0.394	0.401
$q(H_2)$	0.399	0.379	0.387	0.397	0.358

[a] UMP2/6-31G(d,p) results where the total energies in hartrees, the bond lengths in Å, the bond angles in degrees and atomic charges in e are used.
[b] ZPVE (scaled by 0.93).

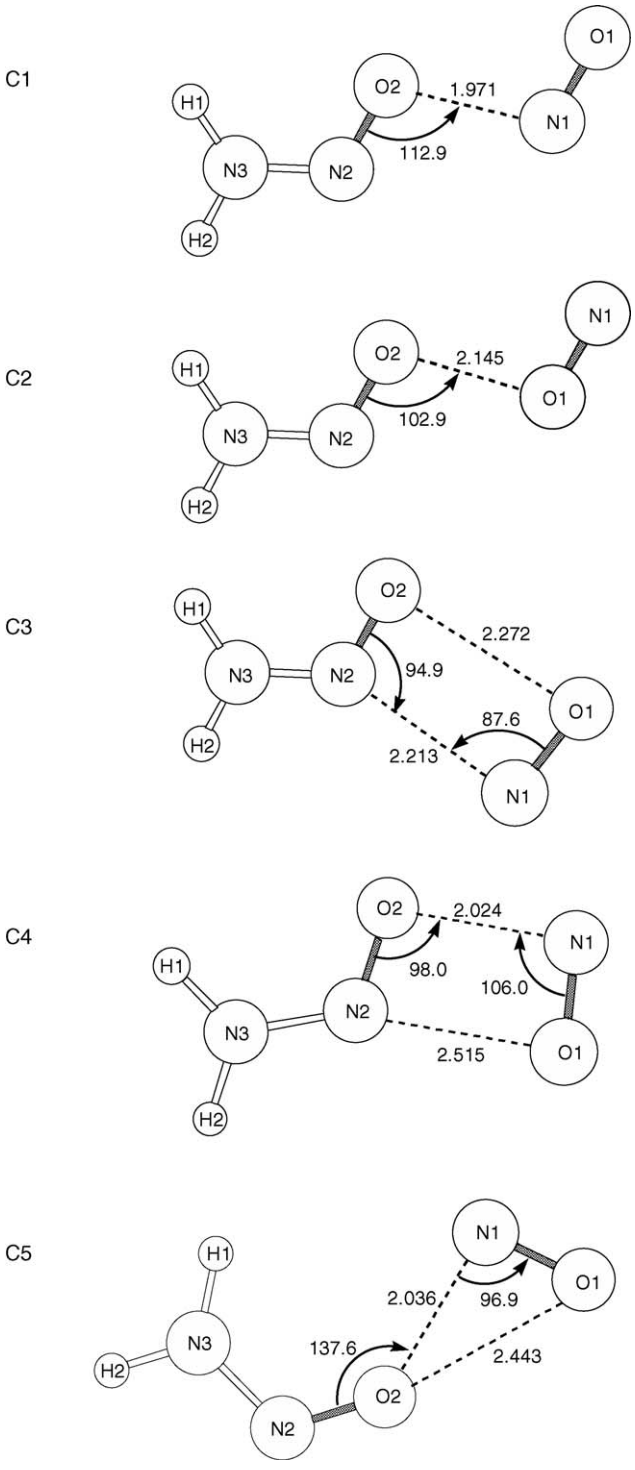

Fig. 3. Optimized structures for the $[NO\cdots H_2NNO]^+$ ion complex obtained by using the MP2/6-31G(d,p) level of theory. The labeling of the atoms in the complexes is consistent with Table 2.

NO moiety (N_1O_1) varies from 75% for C1 to 90% for the C2 structure. In addition, comparison of the geometrical parameters of the isolated NH_2NO molecule (Table 1) and those of NH_2NO moiety in the complex ion (Table 2) indicates that there is little difference between the molecules. Therefore, we feel that it is appropriate to characterize the complex ion $[(NO)_2(NH_2)]^+$, as an ion–dipole complex between NO^+ and the NH_2NO molecule $[NO^+\cdots H_2NNO]$.

The relative energy changes for the dissociation of the five different complexes, which are calculated at the on the MP2/6-31G** level, are summarized in Table 3. Dissociation channel 1, which leads to NO^+ and H_2NNO, is lower in energy than that for the dissociation channel 2, which leads to NO and H_2NNO^+. The calculated dissociation energy through channel 1 for the most stable structure, C4, is found to be 40.19 kcal/mol without correction and 34.48 kcal/mol including corrections (ZPVE and BSSE). This value is larger than that derived from the equation of the bond energy with proton affinity of H_2NNO [67]. The dissociation energy of the C4 complex leading to H_2NNO^+ plus NO is calculated to be 19.31 (without correction) and 23.18 kcal/mol (with correction) *higher* in energy than that for dissociation channel 1. Therefore, based on these calculations, we expect the generation of H_2NNO^+ plus NO to be less efficient than that of NO^+ plus H_2NNO. This result explains why it is very difficult to detect the isolated H_2NNO^+ ion or $[(H_2NNO)(NH_3)_{n-1}]^+$ cluster ions in the NO/NH_3 cluster system.

Lastly, we have also calculated the system of a single ammonia molecule complexed directly either to $[H_2NNO]^+$ or with $[NO\cdots H_2NNO]^+$ for a variety of different configurations. These calculations have been performed at the DFT level of theory using the B3LYP hybrid functional and utilizing the basis set of the 6-31 + G* quality. This level of theory has been proven in the literature as a precise computational approach in calculations involving hydrogen bonds. All calculations have been performed with full geometry optimization in the gas phase and the energies are reported in Tables 4 and 5.

For the $[NH_3\cdots H_2NNO]^+$ system the lowest energy structures are depicted in Fig. 4. Structure D1-A, is the most stable structure, where a NH_4^+ is now generated via proton transfer from the H_2NNO. The electrostatic potential is shown in Fig. 5 and shows the positive charge is indeed localized on the NH_4 moiety.

For the $[NH_3\cdots H_2NNO\cdots NO]^+$ system there are several possible stable forms. One is C4-B (Fig. 6(b)) where the ammonia molecule is directly associated with the NO (i.e., $[H_2NNO\cdots NO\cdots NH_3]^+$). The electrostatic potential for this cluster ion is shown in Fig. 7(b), where the positive charge is equally shared on both the NH_2 and the NH_3. However, a second stable isomer is if the ammonia is instead again adjacent to the NH_2, $[NH_3\cdots H_2NNO\cdots NO]^+$ (C4-A Fig. 6(d)). In this case proton transfer once more occurs creating $[NH_4\cdots HNNO\cdots NO]^+$. The electrostatic potential for this cluster ion is shown in Fig. 7(a), showing again the positive charge is localized on the NH_4^+ cation.

These calculations show that if the ammonia is adjacent to the NH_2 of the H_2NNO molecule then facile proton transfer occurs from the NH_2^+ cation to the NH_3 molecule generating the NH_4^+ cation, This effect is increased by π–π coupling between π electrons of the NH_2^+ cation and π electrons of the NO monomer, resulting in the sp^2 hybridization of the NH_2^+ nitrogen atom, being a proton donor in the proton transfer mechanism.

We note that this effect is also consistent with our mass spectrometric observation. That is, we do not observe cluster ions of

Table 3
Calculated dissociation energies of complexes (in kcal/mol)[a]

	C1	C2	C3	C4	C5
Channel 1[b]	38.67(33.65)	27.57(23.31)	37.17(31.72)	40.19(34.48)	29.45(24.59)
Channel 2[c]	57.97(56.51)	46.88(46.62)	56.48(54.54)	59.50(57.66)	48.75(48.03)

[a] UMP2/6-31G(d,p) results where values in parentheses are corrected by ZPVE and BSSE.
[b] $[NO\cdots H_2NNO]^+ \rightarrow NO^+ + H_2NNO$.
[c] $[NO\cdots H_2NNO]^+ \rightarrow NO + H_2NNO^+$.

Table 4
The energies of the $[NH_3\text{-}NH_2\text{-}(NO)]^+$ complexes (unrestricted B3LYP/6-31 + G*)

$NH_3\text{-}NH_2^+\text{-}NO$ complex	Doublet	
	Energy (hartree)	Energy (kcal/mol)
D1-A	−242.1410	0.0
D1-B	−242.1102	19.3
D1-C	−242.1059	22.0
D1-D	−242.1331	5.0

the type $[H_2NNO\cdots(NH_3)_n]^+$. Presumably, NH_4^+ is generated via proton transfer and the neutral HNNO product then evaporates from the cluster, creating then a neat protonated ammonia cluster $(NH_3)_nH^+$. In contrast, we only observe the H_2NNO specie in clusters that also contain NO. Based on these optimized geometries, the observed $[(H_2NNO)_x(NO)((NH_3)_{n-x}]^+$ peaks where $x = 1$ or 2, must have a structure similar to that of C4-B. That is, the cluster ion must have an NO molecule 'bridging' the H_2NNO and the solvating ammonia's, in order to prevent the facile proton transfer, as seen in C4-A.

Table 5
The energies of the $[NH_3\text{-}NH_2\text{-}(NO)_2]^+$ complexes (unrestricted B3LYP/6-31 + G*)

$NH_3\text{-}NH_2^+(NO)_2$ complex	Singlet	
	Energy (hartree)	Energy (kcal/mol)
C1-A	−372.0649	0.1
C1-B	−372.0604	3.0
C1-C	−372.0473	11.2
C2-A	−372.0347	19.1
C2-B	−372.0383	16.8
C2-C	−372.0540	7.0
C3-A	−372.0644	0.4
C3-B	−372.0414	14.9
C3-C	−372.0552	6.2
C4-A	−372.0651	0.0
C4-B	−372.0622	1.8
C4-C	−372.0464	11.7
C5-A	−372.0493	9.9
C5-B	−372.0383	16.8
C5-C	−372.0565	5.4
C6-A	−372.0600	3.2
C6-B	−372.0605	2.9

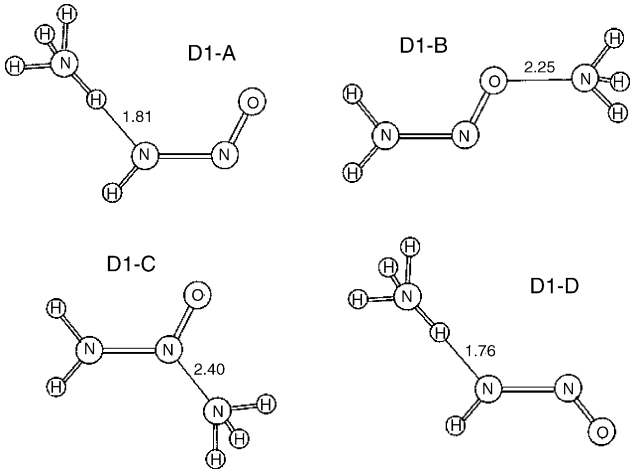

Fig. 4. The geometries of the $[NH_3\cdots H_2NNO]^+$ complexes in the singlet electronic state (unrestricted B3LYP/6-31 + G*).

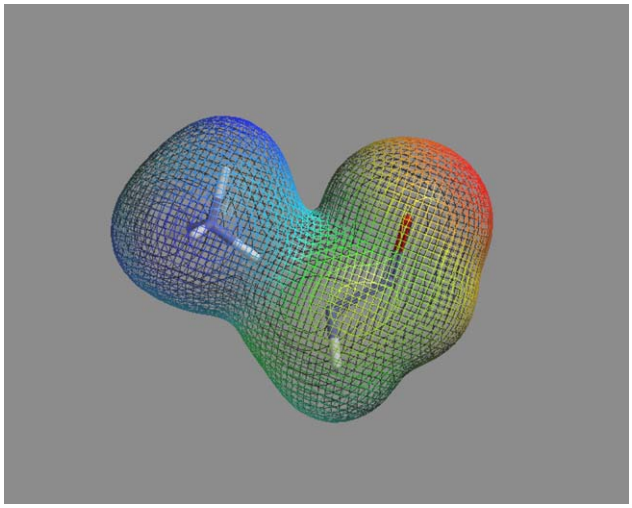

Fig. 5. The electrostatic potential of $[NH_3\cdots H_2NNO]^+$ complex D1-A.

5. Discussion

H_2NNO is recognized to play a decisive role in the $DeNO_x$ process, as mentioned previously in the introduction. The formation of H_2NNO and its relevant chemical reactions have become a subject of tremendous studies, both theoretically [49–53] and experimentally [54–57]. A substantial fraction of the work has been centered mainly on the kinetic and energetic aspects for the reaction between NH_2 and NO, leading to the formation of

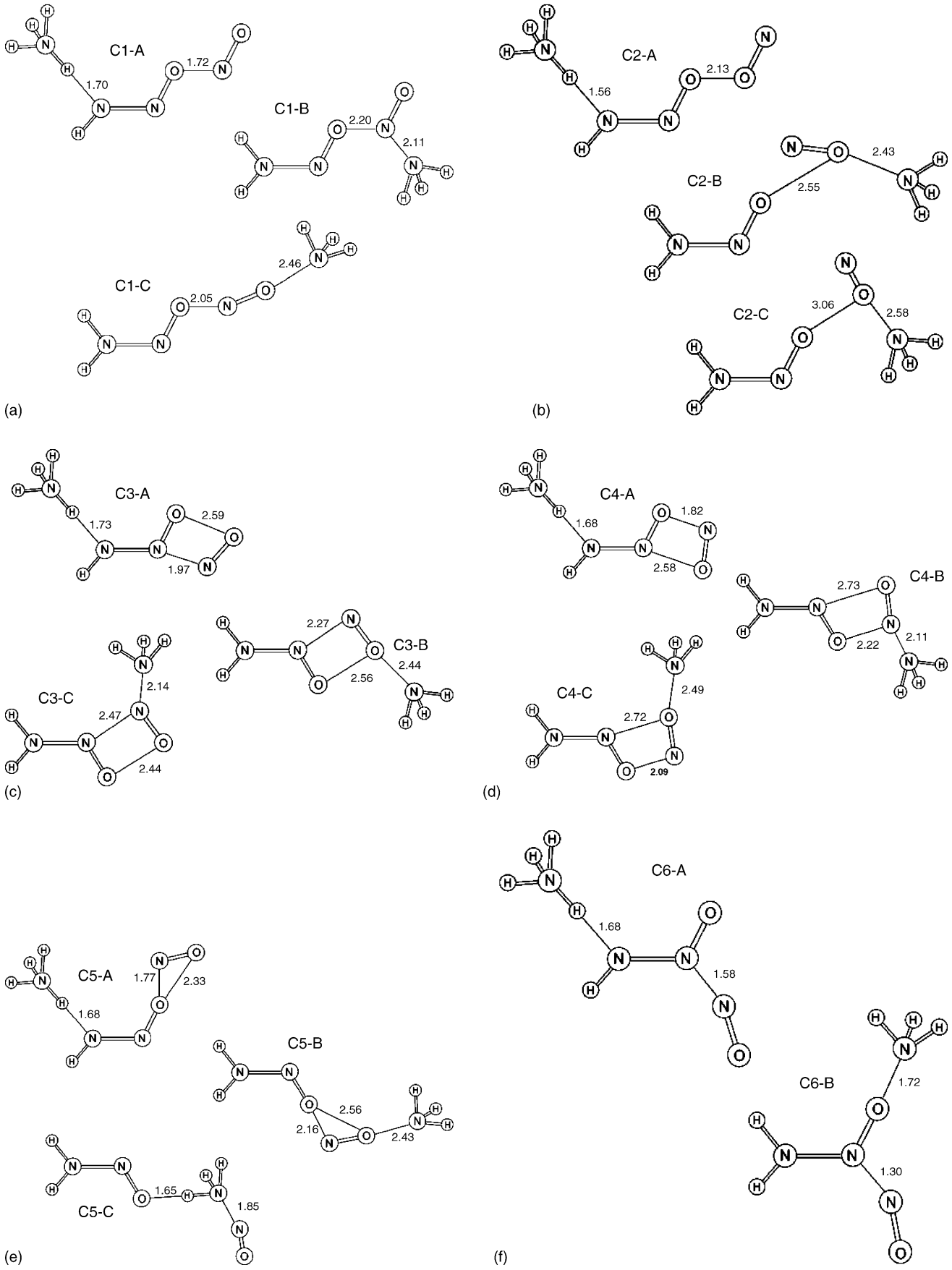

Fig. 6. The geometries of the $[NH_3\cdots H_2NNO\cdots NO]^+$ complexes in the singlet electronic state (unrestricted B3LYP/6-31 + G*).

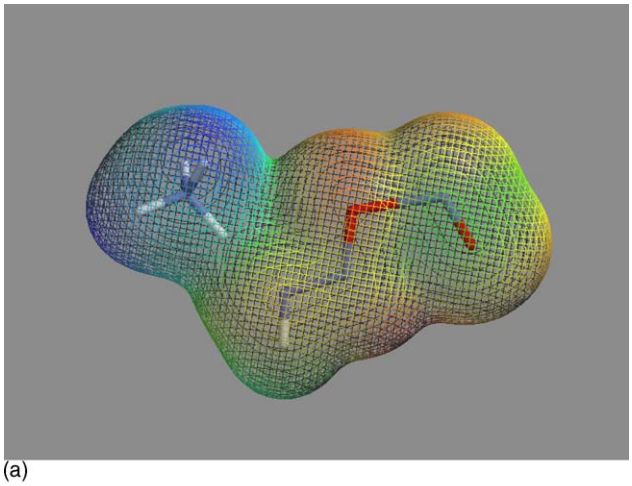
(a)

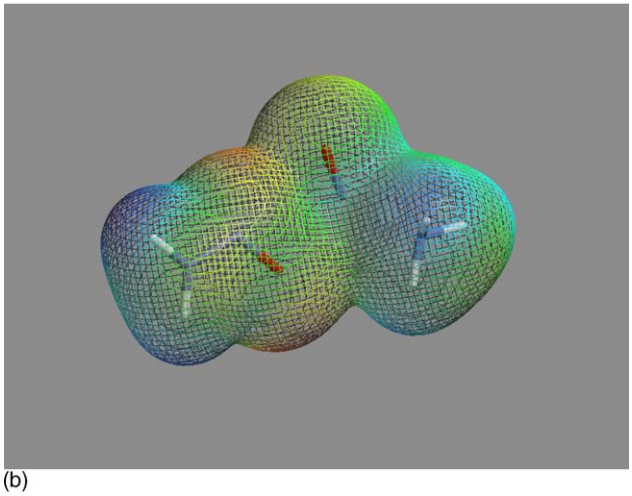
(b)

Fig. 7. (a) The electrostatic potential of $[NH_3\cdots H_2NNO\cdots NO]^+$ complex C4-A. (b) The electrostatic potential of $[H_2NNO\cdots NO\cdots NH_3]^+$ complex C4-B.

either N_2 plus H_2O or HN_2 plus OH. In both cases the formation of H_2NNO is invoked as an intermediate. However, there have only been a few investigations reporting the direct detection of the H_2NNO species experimentally [44,45,58]. The H_2NNO species was observed during the catalytic chemical reaction of NH_3 and NO gas mixtures on vanadium oxide catalysts via mass spectrometry [44]. Matrix infrared study [58] (and ab initio calculation) led to identification of H_2NNO, where the low temperature would prevent rapid dissociation of the H_2NNO species. Lastly, H_2NNO has been generated and characterized in dilute gas mixtures via means of neutralization reionization mass spectrometry [45]. These experimental results appear to be consistent with our present study showing the formation of H_2NNO mediated within a cluster environment.

The chemical reactivity of the $[(NO)_m(NH_3)_n]^+$ cluster ion provides an interesting contrast with that of $[(NO)_m(ROH)_n]^+$. As noted previously, mass spectra for the NO/ROH cluster ion [32–34,41] shows significant formation of the RONO species within these cluster ions. Peaks corresponding to $[(NO)(CH_3ONO)_n]^+$ clusters containing up to $n=12$ are observed over a wide range of mixing concentration of NO/CH_3OH[41].

Table 6
Comparison of the estimated energy changes for the reactions of $(NO)_2$ and $(NO)_3^+$ with CH_3OH or NH_3 to form CH_3ONO or H_2NNO species, respectively[a]

Reactions	ΔE_{rxn}(kcal/mol)
$(NO)_2$[b] + $CH_3OH \rightarrow CH_3ONO + HNO$	14.8
$(NO)_2$[b] + $NH_3 \rightarrow H_2NNO$[c] + HNO	11.9
$(NO)_3^+$[b] + $CH_3OH \rightarrow NO^+\cdots CH_3ONO$[d] + HNO	5.9
$(NO)_3^+$[b] + $NH_3 \rightarrow NO^+\cdots H_2NNO$[d] + HNO	3.4

[a] The heats of formation of some neutral species are taken from Ref. [63], except where indicated.

[b] Estimated on the basis of the reaction: $NO + NO \rightarrow (NO)_2$, $NO^+ + NO \rightarrow (NO)_2^+$ and $(NO)_2^+ + NO \rightarrow (NO)_3^+$. For these reactions, the energy changes are found to be −1.59, −13.79 and −7.36 kcal/mol (see Refs. [64] and [65]), respectively. Combining these values with experimental heats of formation of NO and NO^+ (236 kcal/mol, Ref. [66]), the heats of formation of $(NO)_2$ and $(NO)_3^+$ are evaluated to be 41.6 and 257.8 kcal/mol, respectively.

[c] Ref. [67].

[d] Heat of formation can be estimated by a linear relation correlating the bond energy (BE) with the proton affinities (PA). The relation parameters for $NO^+\cdots X$ were found to be BE = −36.38 + 0.338PA (see Ref. [68]), where the energies are expressed in kcal/mol. For $X = CH_3ONO$ (PA = 192.5 kcal/mol, Ref. [69]) and H_2NNO (PA = 191.3 kcal/mol, Ref. [67]), BE is calculated as 28.7 and 28.3 kcal/mol which give us the heat of formation for $NO^+\cdots CH_3ONO$ and $NO^+\cdots H_2NNO$ corresponding to 191.7 and 226.4 kcal/mol, respectively.

In this manuscript we have presented data consistent with cluster ions having H_2NNO species, formed within the NO/NH_3 system. However, not only are their intensities in trace amounts, as compared to that of $[(NO)(NH_3)_n]^+$ cluster ions, but they are observed only when relatively low concentration of NH_3 exists in the pre-expansion gas mixture. From a comparison of results from these two systems, it is evident that there is a difference in the behavior concerning the formation of the H_2NNO species in NO/NH_3 and the RONO moiety in the NO/ROH systems.

We postulated two possible mechanisms to explain the origin of the formation of the cluster ions under multiphoton ionization (MPI) [59–62]: (i) MPI occurs first, then followed by the subsequent chemical reactions within cluster ions and (ii) photochemical reaction induced upon the excitation of the neutral clusters precedes the ionization. In our previous study where we observed complete conversion of NO/CH_3OH into CH_3ONO clusters, we proposed a concerted mechanism for the formation of CH_3ONO molecules [41]. In this mechanism the CH_3ONO molecule is produced through a one-step reaction pathway mediated by the cluster environment.

Based on these considerations, we have examined the energetics for two sets of the reaction channels leading to H_2NNO in NO/NH_3 and CH_3ONO in NO/CH_3OH clusters through the concerted mechanism. Because of the paucity of information on which of the MPI mechanisms dominates, both the neutral and ionic clusters are considered in Table 6. Interestingly, there does not appear to be a large difference in the energetics between NO/NH_3 and NO/CH_3OH. Furthermore, for both the neutral and ionic clusters, the reaction channels yielding the formation of H_2NNO appears to be more favorable over those producing CH_3ONO, from the thermodynamic point of view. This indicates that the chemical reactivity of the NO moiety toward the N–H bond of NH_3 would be at least similar or superior to that toward

the O–H bond of CH_3OH (or ROH). Therefore, we believe that the efficiency of the formation of mixed clusters of the form $[(NO)_p(NH_3)_q]$ from an expansion of the gas mixture NO and NH_3 is so poor that the intensity of their resulting cluster ions is very low. This propensity is attributed, at least in part, to the delicate interplay of interactions among constituents within the neutral clusters. The binding energy of $(NH_3)_q$ for $2 \leq q \leq 6$ is reported to be in the range 2.8–6.2 kcal/mol [70], while for the dimers $(NO)_2$ and $(CH_3OH)_2$ the binding energy is 1.6 [64] and 2.77 kcal/mol [71], respectively. In this regard, we believe that ammonia molecules preferentially form neutral homogeneous clusters, such that the presence of ammonia hinders the production of the heterocluster ions having two or more NO molecules.

Another possible explanation for the low intensity of the H_2NNO species ions is that the dissociation of the H_2NNO to $H_2O + N_2$ is energetically favored by ~80 kcal/mol [49–53]. The losses due to dissociation can result in a diminished intensity for ions containing the H_2NNO species. Unfortunately, it is very difficult to confirm the occurrence of this dissociation process because of the potential interference of water impurities [42] originating from the gas mixtures, the vacuum chamber and from the gas-handling manifold.

Lastly, a third possibility for the low intensity of the H_2NNO species ions is the facile proton transfer with solvating ammonia. Calculations suggest that the H_2NNO molecule is only stable in clusters containing NO. In such a cluster ion the NO can shield the H_2NNO from the solvating ammonia's such that proton transfer does not occur.

6. Concluding remarks

In this paper, we have investigated the formation of H_2NNO species within NO/NH_3 heterocluster ions, where the cluster environment seems to provide an important influence in stabilizing this species. Analysis of the observed mass spectra for NO/NH_3 clusters leads us to suggest that H_2NNO is formed, via the direct mediation of the cluster environment. That is, NO must be present within the cluster in order for the H_2NNO to be observed. According to ab initio calculations, the structure of the NO/NH_3 cluster ion possessing H_2NNO species is best represented as an ion–dipole complex in which the NO^+ ion is solvated by the H_2NNO and solvent molecules. Should the ammonia be adjacent to the H_2NNO, rapid proton transfer can occur and the cluster ion is not experimentally observed. Further work to elucidate the chemical reactivity to the N–H bond within cluster containing NO molecules is planned by employing other amines, instead of ammonia, i.e., CH_3NH_2, $C_2H_5NH_2$ and their isotopomers.

References

[1] B.J. Finlayson-Pitts, J.N. Pitts Jr., Science 276 (1997) 1045.
[2] P.S. Zurer, Chem. Eng. News Dec. 1 (1997) 23.
[3] R. Atkinson, Atmos. Environ. 34 (2000) 2063.
[4] R.K. Lyon, Environ. Sci. Technol. 21 (1987) 231.
[5] R.A. Perry, D.L. Siebers, Nature 324 (1986) 657.
[6] J. Newhall Pont, A.B. Evans, G.C. England, R.K. Lyon, W.R. Seeker, Environ. Prog. 12 (1993) 140.
[7] V.M. Zamansky, L. Ho, P.M. Maly, W.R. Seeker, Combust. Sci. Technol. 120 (1996) 255.
[8] Y.-H. Cho, H.-M. Chang, KSME Int. J. 11 (1997) 428.
[9] H. Bosch, F. Jansen, Catal. Today 2 (1988) 369.
[10] M. Shelef, Chem. Rev. 95 (1995) 209.
[11] M. Iwamoto, Catal. Today 29 (1996) 29.
[12] P. Forzatti, Catal. Today 62 (2000) 51.
[13] B.M. Penetrante, S.E. Schultheis, Non-thermal Plasma Techniques for Pollution Control: Part A Overview, Fundamentals and Supporting Technologies, Springer-Verlag, Berlin Heidelberg, 1993.
[14] B.M. Penetrante, S.E. Schultheis, Non-thermal Plasma Techniques for Pollution Control: Part B Electron Beam and Electrical Discharge Processing, Springer-Verlag, Berlin Heidelberg, 1993.
[15] B.K. Gullett, P.W. Groff, M.L. Lin, J.M. Chen, J. Air Waste Manage. Assoc. 44 (1994) 1188.
[16] K.-P. Francke, H. Miessner, R. Rudolph, Catal. Today 59 (2000) 411.
[17] R. Slone, M. Ramavajjala, V. Palekar, V. Puchkarev, Pulsed corona plasma technology for the removal of NO_x from diesel exhaust, Society of Automotive Engineers Paper Number 982431, October 1998.
[18] H.-R. Paur, S. Jordan, J. Aerosol Sci. 20 (1989) 7.
[19] B.V. Potapkin, M.A. Deminsky, A.A. Fridman, V.D. Rusanov, in: B.M. Penetrante, S.E. Schultheis (Eds.), Non-thermal Plasma Techniques for Pollution Control: Part A Overview, Fundamentals and Supporting Technologies, Springer-Verlag, Berlin Heidelberg, 1993, p. 91.
[20] H. Matzing, H.-R. Paur, H. Bunz, J. Aerosol Sci. 19 (1988) 883.
[21] H. Matzing, Chemical kinetics of flue gas cleaning by irradiation with electron, in: I. Prigoginem, S.A. Rice (Eds.), Advances in Physical Chemistry, vol. LXXX, John Wiley & Sons, New York, 1991, p. 315.
[22] F.C. Fehsenfeld, M. Mosesman, E.E. Ferguson, J. Chem. Phys. 55 (1971) 2120.
[23] F.C. Fehsenfeld, C.T. Howard, A.L. Schmeltekopf, J. Chem. Phys. 63 (1975) 2835.
[24] L. Angel, A.J. Stace, J. Chem. Phys. 109 (1998) 1713.
[25] B.M. Penetrante, J.N. Bardsley, M.C. Hsiao, Jpn. J. Appl. Phys. 36 (1997) 5007.
[26] H. Egsgaard, L. Carlsen, J.Ø. Madsen, Chem. Phys. Lett. 227 (1994) 33.
[27] M. Richter, R. Eckelt, B. Parlitz, R. Fricke, Appl. Catal. B: Environ. 15 (1998) 129.
[28] A.W. Castleman Jr., P.M. Holland, R.G. Keesee, J. Chem. Phys. 68 (1978) 1760.
[29] A.A. Viggiano, Mass Spectrom. Rev. 12 (1993) 115.
[30] E.E. Ferguson, F. Arnold, Acc. Chem. Res. 14 (1981) 327.
[31] F. Yu, R.P. Turco, B. Karcher, F.P. Schroeder, Geophys. Res. Lett. 25 (1998) 3839.
[32] D.N. Shin, R.L. DeLeon, J.F. Garvey, J. Chem. Phys. 110 (1999) 5564.
[33] D.N. Shin, R.L. DeLeon, J.F. Garvey, J. Am. Chem. Soc. 122 (2000) 11887.
[34] J.P. Charlebois, R.L. DeLeon, J.F. Garvey, J. Phys. Chem. A 104 (2000) 6799.
[35] Y.S. Mok, I.S. Nam, J. Chem. Eng. Jpn. 31 (1998) 391.
[36] M.Y. Lykety, P. Xia, J.F. Garvey, Chem. Phys. Lett. 238 (1995) 54.
[37] D.N. Shin, R.L. DeLeon, J.F. Garvey, J. Phys. Chem. A 102 (1998) 7772.
[38] J.-H. Choi, K.T. Kuwata, B.-M. Hass, Y. Cao, M.S. Johnson, M. Okumura, J. Chem. Phys. 100 (1994) 7153.
[39] L. Angel, A.J. Stace, J. Phys. Chem. A 102 (1998) 3037.
[40] E. Hammam, E.P.E. Lee, J.M. Dyke, J. Phys. Chem. A 104 (2000) 4571.
[41] D.N. Shin, T.R. Furlani, R.L. DeLeon, J.F. Garvey, Int. J. Mass Spectrom. 220 (2002) 145.
[42] The mass spectrum of the pure NO molecule is very similar to that of the purified NO sample explored by Poth et al. [43]. They have shown that there was a big difference in mass spectra patterns between purified and unpurified NO samples. Nevertheless, we cannot completely exclude the possibility of the existence of impurities, i.e. NO_2 and N_2O, present in the commercially available premixed gas of NO in Ar used in this study.

[43] L. Poth, Z. Shi, Q. Zhong, A.W. Castleman Jr., J. Phys. Chem. A 101 (1997) 1099.
[44] M. Farber, S.P. Harris, J. Phys. Chem. 88 (1984) 680.
[45] H. Egsggaard, L. Carlsen, T. Weiske, D. Sulzle, H. Schwarz, Chem. Phys. Lett. 199 (1992) 643.
[46] M.J. Frisch, G.W. Trucks, H.B. Schlegel, P.M.W. Gill, B.G. Johnson, M.A. Robb, J.R. Cheeseman, T. Keith, G.A. Petersson, J.A. Montgomery, K. Raghavachari, M.A. Al-Laham, V.G. Zakrzewski, J.V. Ortiz, J.B. Foresman, J. Cioslowski, B.B. Stefanov, A. Nanayakkara, M. Challacombe, C.Y. Peng, P.Y. Ayala, W. Chen, M.W. Wong, J.L. Andres, E.S. Replogle, R. Gomperts, R.L. Martin, D.J. Fox, J.S. Binkley, D.J. Defrees, J. Baker, J.P. Stewart, M. Head-Gordon, C. Gonzalez, J.A. Pople, Gaussian 94, Revision E.2, Gaussian, Inc., Pittsburgh, PA, 1995.
[47] R.F. Hout, B.A. Levi, W.J. Hehre, J. Comput. Chem. 3 (1982) 234.
[48] S.F. Boys, F. Bernardi, Mol. Phys. 19 (1970) 553.
[49] H. Abou-Rachid, C. Pouchan, M. Chaillet, Chem. Phys. 90 (1984) 243.
[50] L.F. Phillips, Chem. Phys. Lett. 135 (1987) 269.
[51] E.W.-G. Diau, S.C. Smith, J. Phys. Chem. 100 (1996) 12349.
[52] M. Wolf, D.L. Yang, J.L. Durant, J. Phys. Chem. A 101 (1997) 6243.
[53] J.A. Miller, S.J. Klippenstein, J. Phys. Chem. A 104 (2000) 2061.
[54] B. Atakan, A. Jacobs, M. Wahl, R. Weller, J. Wolfrum, Chem. Phys. Lett. 155 (1989) 609.
[55] J.W. Stephens, C.L. Morter, S.K. Farhat, G.P. Glass, R.F. Curl, J. Phys. Chem. 97 (1993) 8944.
[56] M. Votsmeier, S. Song, R.K. Hanson, C.T. Bowman, J. Phys. Chem. A 103 (1999) 1566.
[57] J. Park, M.C. Lin, J. Phys. Chem. A 103 (1999) 8906.
[58] J.N. Crowley, J.R. Sodeau, J. Phys. Chem. 94 (1990) 8103.
[59] A. Gedanken, M.B. Robin, N.A. Kuebler, J. Phys. Chem. 86 (1982) 4096.
[60] J.J. Yang, D.A. Gobeli, M.A. El-Sayed, J. Phys. Chem. 89 (1985) 3426.
[61] J. Purnell, S. Wei, S.A. Buzza, A.W. Castleman Jr., J. Phys. Chem. 97 (1993) 12530.
[62] K.W.D. Ledingham, R.P. Singhal, Int. J. Mass Spectrom. Ion Proc. 163 (1997) 149.
[63] R. Atkinson, D.L. Baulch, R.A. Cox, R.F. Hampson Jr., J.A. Kerr, J. Troe, J. Phys. Chem. Ref. Data 21 (1992) 1125.
[64] S.H. Linn, Y. Ono, C.Y. Ng, J. Chem. Phys. 74 (1981) 3342.
[65] S.R. Desai, C.S. Feigerle, J.C. Miller, J. Chem. Phys. 97 (1992) 1793.
[66] S.G. Lias, J.E. Bartmess, J.F. Liebman, J.L. Holmes, R.D. Levin, W.G. Mallard, J. Phys. Chem. Ref. Data 17 (Suppl. 1) (1988).
[67] M. Aschi, F. Grandinetti, Chem. Phys. Lett. 267 (1997) 98.
[68] H. Wincel, Chem. Phys. Lett. 292 (1998) 193.
[69] S.G. Lias, J.F. Liebman, R.D. Levin, J. Phys. Chem. Ref. Data 13 (1984) 695.
[70] W. Kamke, R. Herrmann, Z. Wang, I.V. Hertel, Z. Phys. D 10 (1988) 491.
[71] A. Bizzarri, S. Stolte, J. Reuss, J.G.C.M. van Duijneveldt-van de Rijdt, F.B. van Duijneveldt, Chem. Phys. 143 (1990) 423.